AGU PUBLICATIONS

Geophysical Research Letters

RESEARCH LETTER
10.1002/2014GL059875

Key Points:
- There is strong anisotropy just outside the boundary of the African LLSVP
- The interior of the African LLSVP is (nearly) isotropic
- The LLSVP may represent a barrier to ambient mantle flow

Supporting Information:
- Readme
- Figure S1
- Figure S2
- Figure S3
- Figure S4
- Figure S5
- Figure S6
- Figure S7
- Table S1

Correspondence to:
C. Lynner,
colton.lynner@yale.edu

Citation:
Lynner, C., and M. D. Long (2014), Lowermost mantle anisotropy and deformation along the boundary of the African LLSVP, *Geophys. Res. Lett.*, *41*, 3447–3454, doi:10.1002/2014GL059875.

Received 11 MAR 2014
Accepted 7 MAY 2014
Accepted article online 10 MAY 2014
Published online 27 MAY 2014

Lowermost mantle anisotropy and deformation along the boundary of the African LLSVP

Colton Lynner[1] and Maureen D. Long[1]

[1]Yale University, New Haven, Connecticut, USA

Abstract Shear wave splitting of SK(K)S phases is often used to examine upper mantle anisotropy. In specific cases, however, splitting of these phases may reflect anisotropy in the lowermost mantle. Here we present SKS and SKKS splitting measurements for 233 event-station pairs at 34 seismic stations that sample D″ beneath Africa. Of these, 36 pairs show significantly different splitting between the two phases, which likely reflects a contribution from lowermost mantle anisotropy. The vast majority of discrepant pairs sample the boundary of the African large low shear velocity province (LLSVP), which dominates the lower mantle structure beneath this region. In general, we observe little or no splitting of phases that have passed through the LLSVP itself and significant splitting for phases that have sampled the boundary of the LLSVP. We infer that the D″ region just outside the LLSVP boundary is strongly deformed, while its interior remains undeformed (or weakly deformed).

1. Introduction

The D″ region, the lowermost 200–300 km of the mantle, displays remarkable properties compared to the lower mantle material above it. It is strongly heterogeneous with respect to seismic velocity structure [e.g., *Garnero and Lay*, 1997] and displays an often complicated discontinuity structure [e.g., *Sidorin et al*., 1999]. In contrast to the bulk of the lower mantle, which is thought to be isotropic [*Meade et al*., 1995], there is evidence that D″ exhibits seismic anisotropy, often in both radial and azimuthal geometries [e.g., *Garnero et al*., 2004; *Panning and Romanowicz*, 2006; *Long*, 2009; *Nowacki et al*., 2010; *Cottaar and Romanowicz*, 2013].

Anisotropy has been documented in many geographic regions of D″; a recent review is given by *Nowacki et al*. [2011]. Most studies that examine D″ anisotropy measure the shear wave splitting of *S*, ScS, or Sdiff phases [e.g., *Garnero et al*., 2004; *Maupin et al*., 2005; *Wookey and Kendall*, 2008; *Cottaar and Romanowicz*, 2013], which propagate nearly horizontally through the D″ layer. Such phases have the advantage of long raypaths through D″, but the use of only (sub) horizontal paths prevents a full characterization of the anisotropic geometry. SK(K)S phases have paths through lowermost mantle that are more vertical (incidence angles of ~30°–55°), potentially providing very different sampling of D″ anisotropy. The splitting of SK(K)S phases is, however, nearly always attributed to upper mantle anisotropy [e.g., *Savage*, 1999]. Several lines of evidence support this interpretation, including the observation that SKS and SKKS arrivals for the same event-station pair usually exhibit similar splitting [*Niu and Perez*, 2004]. In the upper mantle, SKS and SKKS raypaths are very similar (Figure 1), but in the lowermost mantle, they sample very different volumes of D″. For this reason, when marked discrepancies between SKS and SKKS splitting are observed, they are usually attributed to anisotropy in the lowermost mantle [e.g., *James and Assumpçao*, 1996; *Niu and Perez*, 2004; *Vanacore and Niu*, 2011], as the bulk of the lower mantle is isotropic [*Meade et al*., 1995]. Although such discrepancies are rare (less than 5% of the global data set) [*Niu and Perez*, 2004], they have been documented in several regions [e.g., *Wang and Wen*, 2007; *Long*, 2009; *Vanacore and Niu*, 2011; *He and Long*, 2011; *Lynner and Long*, 2012].

The most prominent structures observed in the lower mantle in global *S* wave tomography models are two large low shear velocity provinces (LLSVPs) located in roughly antipodal positions beneath Africa and the Pacific [e.g., *Garnero and McNamara*, 2008]. While the geometry of these structures has been fairly well established via the analysis of waveforms and differential travel times [e.g., *Ritsema et al*., 1998; *To et al*., 2005; *Sun and Miller*, 2013] and cluster analysis of tomographic models [*Lekic et al*., 2012], their origin and implications for lower mantle dynamics remain enigmatic. LLSVPs may represent transient thermochemical structures that are swept into "piles" by subducting slabs [e.g., *McNamara and Zhong*,

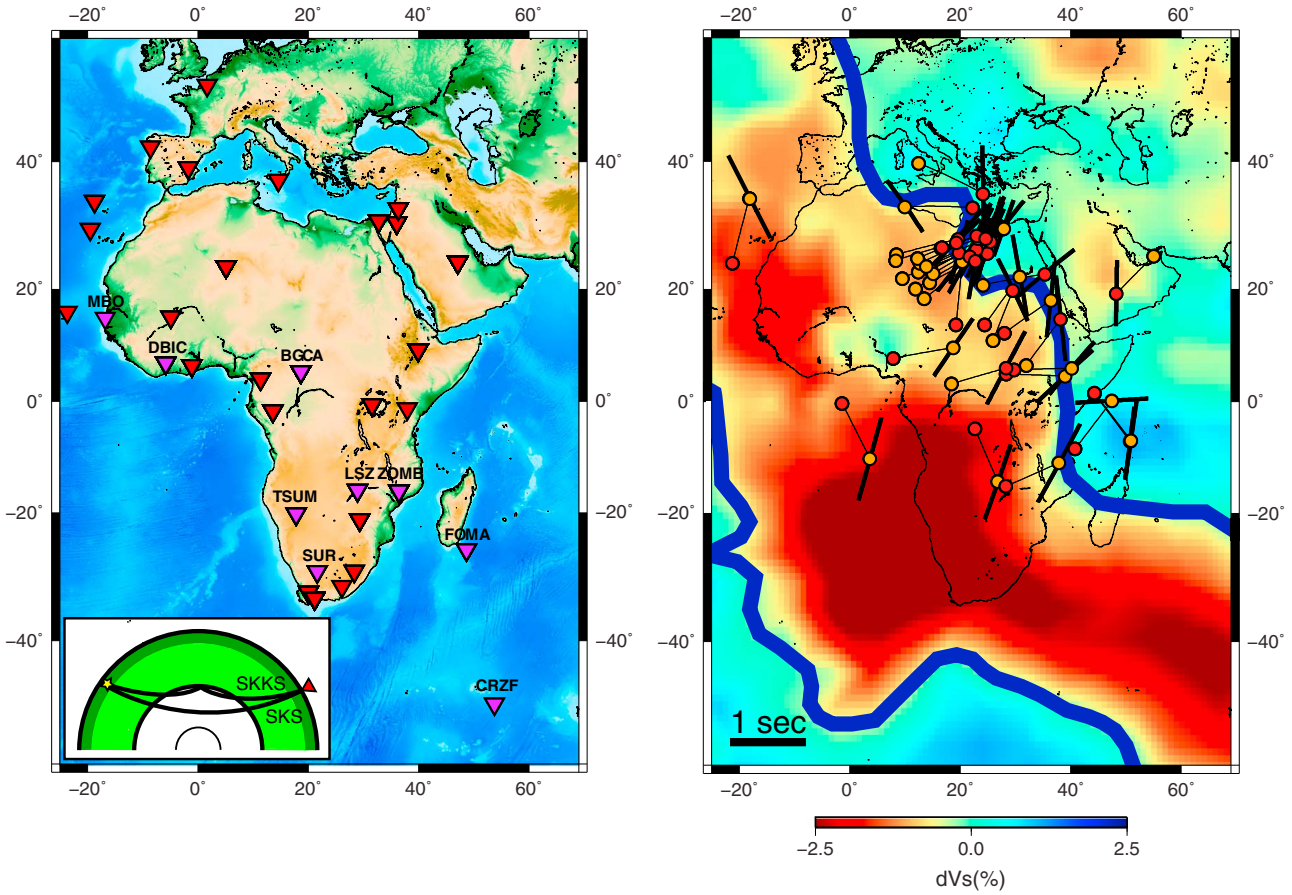

Figure 1. (left) Locations of the 34 seismic stations used in this study (triangles). Stations at which the upper mantle contribution to shear wave splitting can be constrained and removed are labeled and denoted with purple triangles. The inset schematically depicts the different paths that SKS and SKKS phases take through the Earth. (right) All discrepant SKS-SKKS pairs plotted atop the GyPSuM tomography model [*Simmons et al*., 2010]. Red and orange circles denote the phase (red for SKS and orange for SKKS) and are plotted at their pierce points at a depth of 2700 km. Thin lines connect SKS-SKKS pairs. The orientation and length of black bars correspond to measured fast directions and delay times, respectively. Circles with no bars denote null measurements. The boundary of the LLSVP, inferred from the GyPSuM tomography model [*Simmons et al*., 2010], is denoted by the thick blue line.

2005] or long-lived structures that anchor the pattern of mantle convection [*Dziewonski et al*., 2010]. The edges of these structures are sharp [*Ni et al*., 2002] and are often associated with ultralow velocity zones [e.g., *McNamara et al*., 2010]. LLSVP edges may correspond to generation zones for deep mantle plumes [e.g., *Steinberger and Torsvik*, 2012] and the edges of the African LLSVP, in particular, are associated with distinctive anisotropy in the lowermost mantle [*Wang and Wen*, 2007; *Lynner and Long*, 2012; *Cottaar and Romanowicz*, 2013].

The anisotropic structure of the African LLSVP edge has been characterized in a few specific regions, including its eastern [*Wang and Wen*, 2007], southern [*Cottaar and Romanowicz*, 2013], and a small portion of its northern [*Lynner and Long*, 2012] boundaries. Here we present a data set of SKS and SKKS splitting measurements made at stations throughout Africa that features good lowermost mantle sampling of the African LLSVP, including its edges and interior. We identified 233 well-resolved SKS-SKKS pairs at 34 seismic stations for which splitting could be reliably measured; of these, 36 pairs showed discrepant splitting. We restrict our interpretation to SKS-SKKS pairs, as any discrepancies in splitting between the two phases likely reflect an origin in the lowermost mantle. This approach circumvents complications in interpretation of individual splitting measurements due to complex anisotropic structure. We find that SKS-SKKS splitting discrepancies preferentially occur for raypaths that sample the LLSVP boundary, with apparently strong anisotropy just outside the LLSVP border. Most SK(K)S phases that sample the interior of the LLSVP display little or no splitting, likely reflecting nearly isotropic D″ structure.

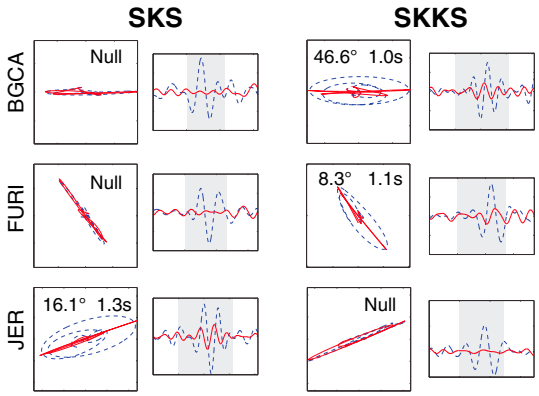

Figure 2. Waveform examples of discrepant pairs of (first and second column) SKS and (third and fourth column) SKKS phases. The first column corresponds to corrected (solid red line) and uncorrected (blue-dashed line) particle motion for the SKS phase with the measured splitting parameters shown. The second column shows the corresponding radial (dashed blue line) and transverse (red line) seismogram components. The third and fourth columns are plotted following the same conventions as the first and second but for the corresponding SKKS phase.

2. Data and Methods

In order to properly characterize both upper and lowermost mantle anisotropy, we examined SK(K)S phases for all events with magnitudes $M_w \geq 5.8$ at epicentral distances between 90° and 130° over the lifetime of the 33 seismic stations examined in this study (Figure 1). All waveforms were band pass filtered to retain energy between 0.04 Hz and 0.125 Hz and visually inspected to ensure good signal-to-noise ratios (SNR). We used the SplitLab software package [*Wüstefeld et al.*, 2008] and simultaneously applied the rotation-correlation and transverse component measurement methods to measure splitting. The rotation-correlation method performs a grid search of possible fast directions and delay times seeking to maximize the cross correlation of the corrected horizontal components, while the transverse component minimization method performs a similar grid search seeking to minimize the energy on the corrected transverse component of the seismogram. The simultaneous use of multiple measurement methods has been shown to produce reliable and reproducible splitting estimates [e.g., *Savage*, 1999; *Lynner and Long*, 2012]. All splitting measurements retained in this data set have 2σ errors of less than ±25° for the fast direction (ϕ) and ±0.7 s for delay time (δt); average errors for the entire data set are ±16.8° and ±0.25 s for ϕ and δt, respectively. Null (that is, nonsplit) arrivals were evaluated based on the linearity of the uncorrected particle motion and SNR. A few stations were found to have improperly aligned horizontal components; we identified and corrected for these misalignments based on polarization analysis of the SK(K)S phases [e.g., *Lynner and Long*, 2012].

In addition to the 33 stations evaluated here, we included measurements from our previous work using identical analysis techniques [*Lynner and Long*, 2012] at seismic station DBIC that met the measurement error criteria used here. After splitting analysis was performed at each station, we focused on those waveforms with either a split or null measurement for both the SKS and SKKS phases for a single event; these represent SKS-SKKS pairs. By restricting our analysis to SKS-SKKS pairs, we take a conservative approach to interpreting lower mantle anisotropy. The use of individual SK(K)S splitting measurements to constrain D″ anisotropy has several pitfalls; in particular, it can be difficult to confidently infer a contribution from anisotropy in the lowermost mantle, instead of the upper mantle [e.g., *Lynner and Long*, 2012]. For SKS-SKKS pairs, in contrast, significant differences in splitting between the two phases for a given event-station geometry indicate a likely contribution from anisotropy in the lowermost mantle, as both phases sample the anisotropic upper mantle in nearly identical ways. We considered a pair discrepant if one phase is null while the other is split, or if the 2σ error spaces for either ϕ or δt are nonoverlapping. If both measurements are null or have overlapping error estimates, they are considered nondiscrepant. Of the waveforms examined in this study, we identified 233 SKS-SKKS pairs, of which 36 were found to have discrepant splitting. Waveform examples of discrepant pairs are shown in Figure 2, while nondiscrepant examples are shown in Figures S1 and S2 (in the supporting information). Event and station information for all SKS-SKKS pairs, along with splitting parameters and error estimates, can be found in the supporting information.

3. Results

In order to visualize our splitting measurements in relation to the (isotropic) velocity structure of the lowermost mantle, we show our results (plotted at the 2700 km depth pierce point for each phase) in map view in Figures 1 and 3. We plot our results atop the GyPSuM *S* wave tomography model [*Simmons et al.*, 2010] in Figure 1. It is also useful to visualize our measurements in the context of many different tomography

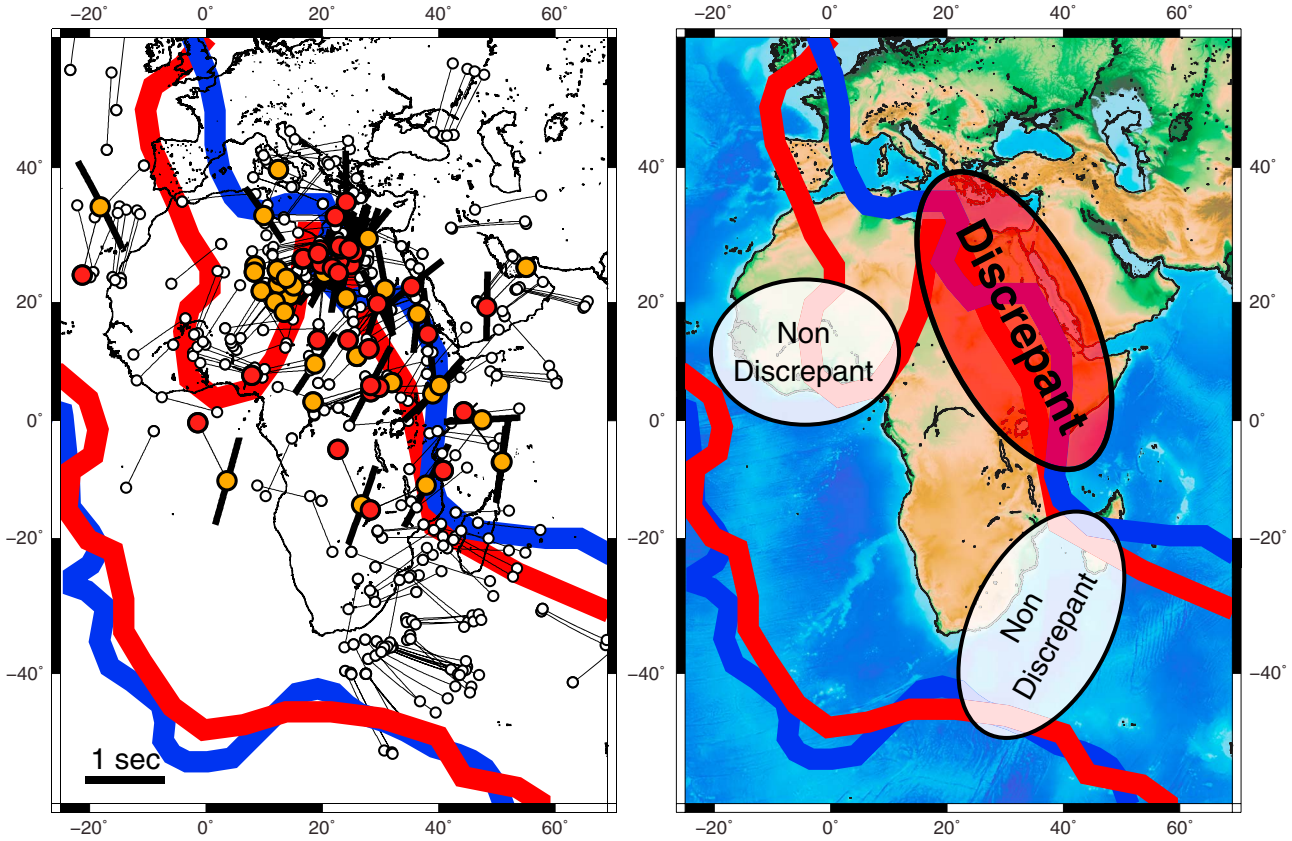

Figure 3. (left) All SKS-SKKS pairs plotted at 2700 km pierce points. Red and orange circles denote the phase for discrepant pairs, as in Figure 1. All nondiscrepant pairs are shown as white circles. Thin lines connect SKS-SKKS pairs. The orientation and length of black bars correspond to measured fast directions and delay times, respectively; only splitting of discrepant pairs is shown. (right) Schematic interpretation of the broad geographic distribution of discrepant (red region) and nondiscrepant (white regions) splitting. The boundaries of the LLSVP inferred from the lower mantle cluster analysis [*Lekic et al.*, 2012] (red line) and from the GyPSuM tomography model [*Simmons et al.*, 2010] (blue line) are shown in each panel.

models. This is easily accomplished using the lower mantle cluster analysis of *Lekic et al.* [2012], which compares the extent of the slow velocity anomaly beneath Africa from five different *S* velocity models (for details, see *Lekic et al.* [2012]). This cluster analysis demonstrates that with the exception of the northern region, the shape and extent of the inferred boundary of the LLSVP are very consistent among the different models (Figure S3 in the supporting information).

Immediately apparent in Figures 1 and 3 is the tendency for the discrepant SKS-SKKS pairs to cluster around the edges of the LLSVP, with only a few discrepancies occurring within the LLSVP itself. Conversely, there are large regions both within and outside the LLSVP itself that are dominated by nondiscrepant pairs (particularly in the southern portion of the study area). This is clear both with respect to the GyPSuM tomography model [*Simmons et al.*, 2010] (Figure 1) and the lower mantle cluster analysis of *Lekic et al.* [2012] (Figure S3). The nondiscrepant regions are dominated by null splitting measurements. One observation worth noting is that within regions sampled by discrepant SKS-SKKS pairs, we often observe nondiscrepant SKS-SKKS pairs as well. However, the discrepant and nondiscrepant raypaths are typically not identical, and usually sample slightly different volumes of mantle or propagate at slightly different azimuths (Figures 3 and 4). This type of pattern may indicate heterogeneity of anisotropic structure on fairly short length scales [e.g., *He and Long*, 2011].

4. Discussion

Discrepant SKS-SKKS splitting is typically interpreted as an anisotropic signal from the lowermost mantle [e.g., *Niu and Perez*, 2004], but other factors may contribute, including crustal anisotropy, heterogeneous anisotropy in the upper mantle or transition zone, or finite-frequency effects. Crustal anisotropy is potentially

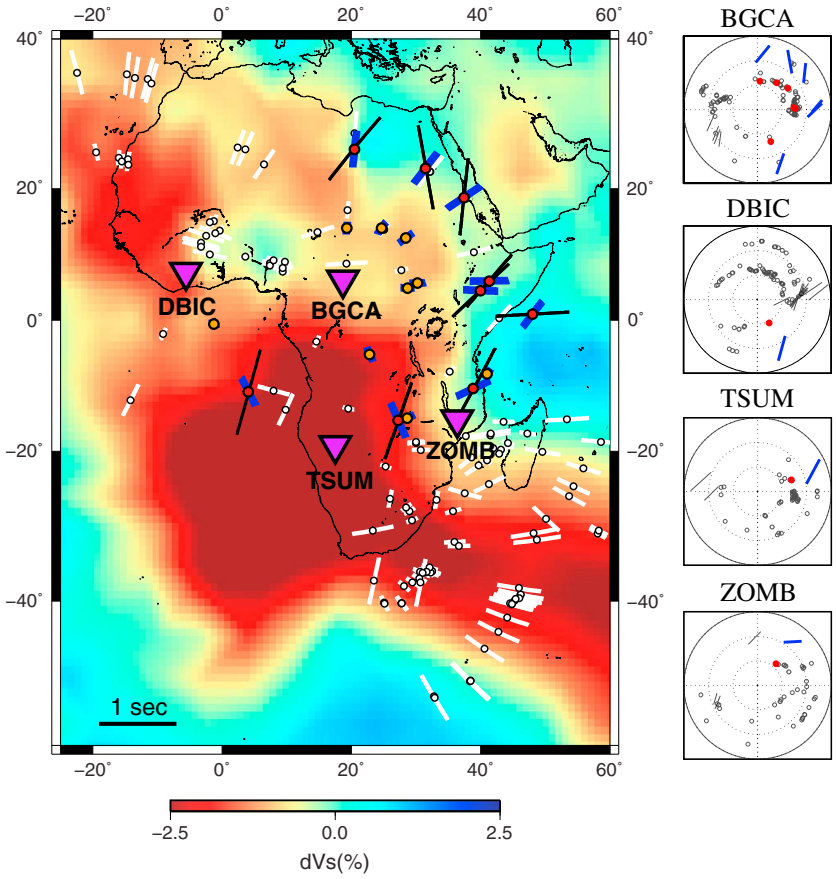

Figure 4. (left) Splitting parameters directly attributed to lowermost mantle anisotropy, from all SKS-SKKS pairs measured at stations with well-constrained upper mantle splitting patterns (triangles). The portion of the raypath that samples D″ (from the CMB to 2600 km depth) for each phase is shown by thick lines (blue for discrepant pairs and white for nondiscrepant pairs). Splitting parameters (black lines) are plotted following the conventions of Figure 3. (right) Stereographic plots of SK(K)S splitting at four stations with simple upper mantle splitting patterns at which discrepant pairs were recorded. Splitting measurements are plotted as a function of incidence angle and backazimuth. Circles denote null splitting measurements and bars denote split measurements with fast direction and delay time shown by the orientation and length of the bars, respectively. Discrepant pairs are highlighted in red (nulls) and blue (splits). The pattern documented at station DBIC is discussed in detail in *Lynner and Long* [2012].

highly heterogeneous and may affect SKS and SKKS phases differently, but delay times due to crustal splitting are usually small (~0.1 s), with few exceptions [e.g., *Kaviani et al.*, 2011]. The pronounced SKS-SKKS discrepancies documented here would require unrealistically strong and heterogeneous crustal anisotropy for their primary origin to be in the crust. Another potential source of discrepant splitting is heterogeneous anisotropic structure in the upper mantle or transition zone. This too is unlikely as a first-order contribution to this data set; Fresnel zones of waves with characteristic periods of ~10 s, such as the SKS and SKKS phases used in this study, overlap substantially in the upper mantle and transition zone for a pair of SKS and SKKS phases. For SKS-SKKS discrepancies to have their primary source in the upper mantle, unrealistically dramatic lateral heterogeneity in anisotropic structure would be required [e.g., *Lynner and Long*, 2012]. Recent work has shown that a full consideration of finite-frequency effects may make a modest contribution to differences in measured SKS-SKKS splitting parameters even for simple upper mantle anisotropic models [*Lin et al.*, 2014], but the effects are small at the epicentral distances relevant for this study (~99°–122°).

Scattering due to isotropic structure in the lowermost mantle may result in energy on the transverse component seismograms that can be mistaken for shear wave splitting. We performed two tests to rule out this effect. First, we reexamined all discrepant pairs using a different filtering scheme that included higher frequencies (0.05 Hz to 0.5 Hz) and found that splitting discrepancies are not strongly affected by frequency

content (Figure S4 in the supporting information). We would expect scattering due to isotropic structure to be highly dependent on frequency. Second, we examined the shape of the transverse component waveforms and confirmed that they are similar to the radial component derivative, rather than the radial component itself, consistent with splitting due to anisotropy rather than scattering (Figure S5 in the supporting information). The most likely primary source of the SKS-SKKS discrepancies documented in this study, therefore, is anisotropy in the lowermost mantle; at the base of the mantle, SKS and SKKS phases sample very different regions (with no overlap in Fresnel zones), and the bulk of the overlying lower mantle is generally thought to be isotropic [*Meade et al*., 1995].

The geographic pattern of SKS-SKKS discrepancies shown in Figures 1 and 3 suggests a contribution to SK(K)S splitting from anisotropic structure in D″ surrounding the African LLSVP. One question, however, is whether the observations require a contrast in anisotropy across the LLSVP boundary, or whether the data could be explained by homogenous anisotropic structure, with discrepant splitting due to the different path lengths and incidence angles of SKS and SKKS phases in the lowermost mantle. For the epicentral distances used in this study, SKKS phases have a shallower incidence angle (by ~ 25°) and therefore longer paths through D″ than the corresponding SKS phases. This difference may result in discrepant splitting, although the differences in observed splitting parameters should be modest unless the anisotropy is very strong. In any case, this is not a viable explanation for this data set, as we generally find that the split phase of the discrepant pairs is not restricted to either SKS or SKKS. Rather, both phases record split and null measurements, particularly along the northern LLSVP boundary (Figures 1 and 3). Instead, the observation of discrepant splitting seems to be controlled by geographic sampling, with D″-associated splitting attributed to waves that sample the lowermost mantle just outside the LLSVP, and little or no splitting generally attributed to waves that sample the LLSVP interior.

While SKS-SKKS discrepancies indicate some contribution from anisotropy in the lowermost mantle, in order to directly constrain the splitting parameters due to D″ anisotropy we must explicitly correct for the splitting due to upper mantle anisotropy beneath any given station. Unfortunately, it is difficult to accurately carry out such a correction for the case of complex upper mantle anisotropy (e.g. multiple layers or a nonhorizontal symmetry axis). Figure S6 (in the supporting information) shows the SK(K)S splitting patterns as a function of backazimuth measured at the 12 stations which show discrepant SKS-SKKS pairs. It is clear that most stations show complex splitting patterns in which measured fast directions and delay times vary with backazimuth; in such cases, we cannot confidently correct for apparent splitting due to upper mantle anisotropy.

At a subset of the stations used in this study, however, the upper mantle splitting signal is sufficiently simple to accurately account for upper mantle anisotropy (BGCA, CRZF, DBIC, FOMA, LSZ, MBO, SUR, TSUM, and ZOMB; Figure 1). At all such stations, we observe predominantly null SK(K)S arrivals across most backazimuths, with very few split SK(K)S phases (Figure S6 in the supporting information). The few split arrivals at these stations are often part of a discrepant SKS-SKKS pair and most likely reflect a contribution from lowermost mantle anisotropy [e.g., *Lynner and Long*, 2012] or are very sparse and do not agree with the overall pattern of observed SK(K)S null splitting (see *Lynner and Long* [2013] for a more detailed discussion). The splitting patterns at these stations are consistent with an apparently isotropic upper mantle; therefore, we can directly associate the measured splitting parameters for the discrepant pairs to the lowermost mantle, with no need for an explicit upper mantle correction (Figure 4). When restricted to such stations, the data set reduces to 9 discrepant and 61 nondiscrepant pairs; six of the nine split arrivals sample the lowermost mantle within 150 km of the boundary of the LLSVP (Figure S7 in the supporting information). In general, these measurements exhibit null splitting for phases that sample the interior of the LLSVP, with observable splitting for phases that sample just outside the LLSVP boundary (Figures 4 and S7). To test the significance of this result, we evaluated a "null hypothesis" model in which we randomly assigned the locations of the nine discrepant splits within the spatial distribution of the actual data and found that our observation of discrepant splits clustering near the LLSVP boundary (Figure S7) is statistically significant ($p = <0.05$).

We propose, therefore, that the lowermost mantle within the LLSVP itself is isotropic or nearly so (or in a geometry that would not affect the splitting of SK(K)S phases), while the mantle just outside the LLSVP exhibits much stronger anisotropy; to account for the (on average) 0.9 s of delay time observed in these pairs, ~2% anisotropy is required for a 200 km thick anisotropic region along the boundary. *Wang and Wen* [2007]

and *Cottaar and Romanowicz* [2013] recently proposed similar scenarios for the eastern and southern edges of the African LLSVP, respectively. In the scenario proposed by *Wang and Wen* [2007], however, the anisotropic region extends into the southern portion of the LLSVP where we observe many nondiscrepant pairs. This is potentially due to different methodologies; we use only SKS-SKKS pairs while *Wang and Wen* [2007] use all SK(K)S splitting for which they believe upper and lowermost mantle signals can be constrained.

Our observations suggest a dramatic change in the anisotropic structure across the boundary of the African LLSVP, which may reflect changes in mineralogy (e.g., perovskite versus post-perovskite), in deformation mechanism (e.g., dislocation versus diffusion creep), or a contrast in the amount of deformation (strong deformation just outside the boundary versus little or no deformation within the LLSVP itself). The mechanism for D″ anisotropy remains unclear, with possible contributions from the lattice preferred orientation (LPO) of perovskite, post-perovskite, and/or ferropericlase or from the shape preferred orientation (SPO) of partial melt or other materials (see *Nowacki et al*. [2011], for a recent review). Recent forward modeling work by *Ford et al*. [2013] suggests that the geometry of D″ anisotropy just outside the northeastern edge of the African LLSVP is most consistent with the (nonhorizontal) alignment of post-perovskite.

Regardless of the exact mechanism for anisotropy, our measurements, in combination with other observations beneath Africa [*Wang and Wen*, 2007; *Cottaar and Romanowicz*, 2013], are most consistent with a scenario in which deformation (and thus strongly anisotropic structure) is concentrated along the boundaries of LLSVP structures in the lowermost mantle. Our measurements of null splitting from multiple azimuths for a region within the southern portion of the LLSVP (Figure 4) are particularly consistent with lowermost mantle isotropy (or weak anisotropy) within the LLSVP boundary, with abundant evidence for a contribution to SK(K)S splitting from strong anisotropy just outside the boundary. This interpretation suggests, in turn, that LLSVPs represent lower mantle structures that are resistant to deformation and may act to deflect or impede ambient mantle flow, leading to particularly strong D″ anisotropy just outside their edges.

5. Summary

We examined shear wave splitting of SK(K)S phases at 34 seismic stations that sample the lowermost mantle in and around the African LLSVP. We identified 36 SKS-SKKS pairs that exhibit well-resolved, strongly discrepant splitting. The vast majority of discrepant SKS-SKKS pairs sample the lowermost mantle near the border of the LLSVP, while nondiscrepant pairs tend to sample its interior or the region far outside the LLSVP (with a few exceptions). For phases recorded at stations with a well-constrained upper mantle splitting contribution, we can generally rule out splitting of phases that sample the lowermost mantle within the LLSVP, while corresponding phases that sample just outside along the boundary of the LLSVP are generally split. We hypothesize that interior of the LLSVP is (nearly) isotropic, while there is strong anisotropy just outside the LLSVP boundary. This suggests that lowermost mantle deformation is concentrated just outside the boundary of the LLSVP, while its interior remains undeformed (or only weakly deformed). This scenario is consistent with the idea that LLSVPs represent major, long-lived lower mantle structures that are resistant to internal deformation. We hypothesize that these structures may represent barriers to ambient mantle flow, acting to deflect flow and concentrate deformation at their boundaries.

Acknowledgments

This work was funded by NSF grant EAR-1150722. Figures were prepared using Generic Mapping Tools [*Wessel and Smith*, 1991]. Seismic data from the Global Seismograph Network (II, IU), Global Telemetered Seismic Network (GT), Geoscope (G), Geofon (GE), Mednet (MN), the Portuguese National Seismic Network (PM), and the Africa Array (AF) were accessed via the Data Management Center (DMC) of the Incorporated Research Institutions for Seismology (IRIS). We are grateful to Sanne Cottaar and an anonymous reviewer for insightful comments that improved the paper.

The Editor thanks Sanne Cottaar and an anonymous reviewer for their assistance in evaluating this paper.

References

Cottaar, S., and B. Romanowicz (2013), Observations of changing anisotropy across the southern margin of the African LLSVP, *Geophys. J. Int.*, *195*(2), 1184–1195.

Dziewonski, A. M., V. Lekic, and B. Romanowicz (2010), Mantle anchor structure: An argument for bottom up tectonics, *Earth Planet. Sci. Lett.*, *299*, 69–79.

Ford, H. A., M. D. Long, C. Lynner, and X. He (2013), Forward modeling of observations of shear wave splitting along the edge of the African LLSVP: Implications for flow in the deep mantle, AGU Fall Meeting Abstract DI41B-06.

Garnero, E., and T. Lay (1997), Lateral variations in lowermost mantle shear wave anisotropy, *J. Geophys. Res.*, *102*, 8121–8135, doi:10.1029/96JB03830.

Garnero, E. J., and A. McNamara (2008), Structure and dynamics of Earth's lower mantle, *Science*, *320*, 626–628.

Garnero, E. J., V. Maupin, T. Lay, and M. J. Fouch (2004), Variable azimuthal anisotropy in Earth's lowermost mantle, *Science*, *306*, 259–261.

He, X., and M. D. Long (2011), Lowermost mantle anisotropy beneath the northwestern Pacific: Evidence from ScS, PcS, SKS, and SKKS phases, *Geochem. Geophys. Geosyst.*, *12*, Q12012, doi:10.1029/2011GC003779.

James, D. E., and M. Assumpçao (1996), Tectonic implications of S-wave anisotropy beneath SE Brazil, *Geophys. J. Int.*, *126*, 1–10.

Kaviani, A., G. Rümpker, M. Weber, and G. Asch (2011), Short-scale variations of shear-wave splitting across the Dead Sea basin: Evidence for the effects of sedimentary fill, *Geophys. Res. Lett.*, *38*, L04308, doi:10.1029/2010GL046464.

Lekic, V., S. Cottaar, A. M. Dziewonski, and B. Romanowicz (2012), Cluster analysis of global lower mantle tomography: A new class of structure and implications for chemical heterogeneity, *Earth Planet. Sci. Lett.*, *357–358*, 68–77.
Lin, Y.-P., L. Zhao, and S.-H. Hung (2014), Full-wave effects on shear wave splitting, *Geophys. Res. Lett.*, *41*, 799–804, doi:10.1002/2013GL058743.
Long, M. D. (2009), Complex anisotropy in D″ beneath the eastern Pacific from SKS-SKKS splitting discrepancies, *Earth Planet. Sci. Lett.*, *285*, 181–189.
Lynner, C., and M. D. Long (2012), Evaluating contributions to SK(K)S splitting from lower mantle anisotropy: A case study from station DBIC, Côte D'Ivoire, *Bull. Seismol. Soc. Am.*, *102*, 1030–1040.
Lynner, C., and M. D. Long (2013), Sub-slab seismic anisotropy and mantle flow beneath the Caribbean and Scotia subduction zones: Effects of slab morphology and kinematics, *Earth Planet. Sci. Lett.*, *361*, 367–378.
Maupin, V., E. J. Garnero, T. Lay, and M. J. Fouch (2005), Azimuthal anisotropy in the D″ layer beneath the Caribbean, *J. Geophys. Res.*, *110*, B08301, doi:10.1029/2004JB003506.
McNamara, A. K., and S. Zhong (2005), Thermochemical structures beneath Africa and the Pacific Ocean, *Nature*, *437*, 1136–1139, doi:10.1038/nature04066.
McNamara, A. K., E. J. Garnero, and S. Rost (2010), Tracking deep mantle reservoirs with ultra-low velocity zones, *Earth Planet. Sci. Lett.*, *299*, 1–9, doi:10.1016/j.epsl.2010.07.042.
Meade, C., P. G. Silver, and S. Kaneshima (1995), Laboratory and seismological observations of lower mantle isotropy, *Geophys. Res. Lett.*, *22*, 1293–1296, doi:10.1029/95GL01091.
Ni, S., E. Tan, M. Gurnis, and D. Helmberger (2002), Sharp sides to the African superplume, *Science*, *296*, 1850–1852.
Niu, F., and A. M. Perez (2004), Seismic anisotropy in the lower mantle: A comparison of waveform splitting of SKS and SKKS, *Geophys. Res. Lett.*, *31*, L24612, doi:10.1029/2004GL021196.
Nowacki, A., J. Wookey, and J. M. Kendall (2010), Deformation of the lowermost mantle from seismic anisotropy, *Nature*, *467*, 1091–1094.
Nowacki, A., J. Wookey, and J. M. Kendall (2011), New advances in using seismic anisotropy, mineral physics and geodynamics to understand deformation in the lowermost mantle, *J. Geodyn.*, *52*, 205–228.
Panning, M., and B. Romanowicz (2006), A three-dimensional radially anisotropic model of shear velocity in the whole mantle, *Geophys. J. Int.*, *167*, 361–379.
Ritsema, J., S. Ni, D. V. Helmberger, and H. P. Crotwell (1998), Evidence for strong shear velocity reductions and velocity gradients in the lower mantle beneath Africa, *Geophys. Res. Lett.*, *25*, 4245–4258.
Savage, M. K. (1999), Seismic anisotropy and mantle deformation: What have we learned from shear wave splitting?, *Rev. Geophys.*, *37*, 65–106.
Sidorin, I., M. Gurnis, and D. V. Helmberger (1999), Evidence for a ubiquitous seismic discontinuity at the base of the mantle, *Science*, *286*, 1326–1331.
Simmons, N. A., A. Forte, L. Boschi, and S. Grand (2010), GyPSuM: A joint tomographic model of mantle density and seismic wave speeds, *J. Geophys. Res.*, *115*, B12310, doi:10.1029/2010JB007631.
Steinberger, B., and T. H. Torsvik (2012), A geodynamic model of plumes from the margins of large low shear velocity provinces, *Geochem. Geophys. Geosyst.*, *13*, Q01W09, doi:10.1029/2011GC003808.
Sun, D., and M. S. Miller (2013), Study of the western edge of the African large low shear velocity province, *Geochem. Geophys. Geosyst.*, *14*, 3109–3125, doi:10.1002/ggge.20185.
To, A., B. Romanowicz, Y. Capdeville, and N. Takeuchi (2005), 3D effects of sharp boundaries at the borders of the African and Pacific Superplumes: Observation and modeling, *Earth Planet. Sci. Lett.*, *233*, 137–153.
Vanacore, E., and F. Niu (2011), Characterization of the D″ layer beneath the Galapagos Islands using SKKS and SKS waveforms, *Earthquake Sci.*, *24*, 87–99.
Wang, Y., and L. Wen (2007), Complex seismic anisotropy at the border of a very low velocity province at the base of the Earth's mantle, *J. Geophys. Res.*, *112*, B09305, doi:10.1029/2006JB004719.
Wessel, P., and W. H. F. Smith (1991), Free software helps map and display data, *Eos Trans. AGU*, *72*, 441–446, doi:10.1029/90EO00319.
Wookey, J., and J. M. Kendall (2008), Constraints on lowermost mantle mineralogy and fabric beneath Siberia from seismic anisotropy, *Earth Planet. Sci. Lett.*, *275*, 32–42.
Wüstefeld, A., G. Bokelmann, G. Barruol, and C. Zaroli (2008), Splitlab: A shear-wave splitting environment in Matlab, *Comput. Geosci.*, *34*, 515–528.